



# Molecular dynamics method to predict the effects of temperature and strain rate on mechanical properties of Aluminum/Copper superalloy

Mostafa Yazdani<sup>1,2</sup> · Aazam Ghassemi<sup>1,2</sup> · Mohamad Shahgholi<sup>1,2</sup> · Javad Jafari Fesharaki<sup>1,2</sup> · Seyed Ali Galehdari<sup>1,2</sup>

Received: 19 December 2024 / Accepted: 5 March 2025

© The Author(s), under exclusive licence to Springer-Verlag GmbH Germany, part of Springer Nature 2025

## Abstract

Metal alloys are engineered materials designed to enhance mechanical performance. Achieving optimal mechanical properties through alloy composition has been the focus of extensive research. This study employs the meshless molecular dynamics method to investigate the influence of temperature, strain rate, and copper content on the mechanical properties of Aluminum/Copper (Al-Cu) superalloy. The research focuses on the variation of copper content from 1 to 20%, temperature from 300 to 600 K, and strain rates between  $0.001 \text{ ps}^{-1}$  and  $0.01 \text{ ps}^{-1}$ , assessing their impact on the ultimate tensile strength (UTS) and elastic modulus of the alloy. The results show a significant enhancement in both UTS and elastic modulus with increasing copper content, with the UTS increasing by 359% and the elastic modulus by 281% when copper content rises from 1 to 20%. In contrast, increasing the temperature from 300 to 600 K results in a 31% reduction in UTS and an 18.9% decrease in elastic modulus, highlighting the sensitivity of these properties to thermal effects. Additionally, higher strain rates were found to improve both UTS and elastic modulus, with an 11.95% increase in UTS and an 8.34% increase in elastic modulus at the highest strain rate ( $0.01 \text{ ps}^{-1}$ ). These findings demonstrate the critical role of alloy composition, temperature, and strain rate in tailoring the mechanical properties of Al-Cu alloys, providing insights for optimizing the material for high-performance applications.

**Keywords** Molecular dynamics method · Al-Cu alloy · Elastic modulus · Stress–strain curve

## Introduction

Today, alloys and superalloys have garnered significant interest from scientists worldwide. Extensive experimental and theoretical studies have been conducted on alloys, including the design of new types of superalloys using additive fabrication [1], phase prediction [2], the formation of low-angle grain boundaries [3, 4], and the development of high-temperature alloys [5]. Additionally, other studies

have investigated alloys and their mechanical and physical properties [6–10].

Wang et al. [11] examined the mechanical characteristics of aluminum-copper alloys using the wire and arc additive manufacturing technique to achieve enhanced and more isotropic mechanical properties. Their research reported an elastic modulus of 96 GPa and an ultimate strength of 260 MPa. Mair et al. [12] investigated the mechanical and structural properties of aluminum-copper alloys using the laser powder-bed fusion method. A small number of other elements, such as Mn, Cr, and Ti, was incorporated into the alloy. Stress–strain diagrams were obtained through tensile testing in an orientation perpendicular to the structure. The ultimate tensile strength (UTS) of this structure was reported to range from 300 to 350 MPa.

Milligan et al. [13] examined the influence of alloy morphology and matrix crystallographic orientation on strain-hardening behavior, as well as the impact of heat treatment on material characteristics. Their results showed that increasing the temperature up to 305°C caused the yield strength to decline from 365 to 95 MPa.

✉ Aazam Ghassemi  
a\_ghassemi@iau.ac.ir

Mohamad Shahgholi  
Mohamad.shahgholi@iau.ac.ir

<sup>1</sup> Department of Mechanical Engineering, Najafabad Branch, Islamic Azad University, Najafabad, Iran

<sup>2</sup> Modern Manufacturing Technologies Research Center, Department of Mechanical Engineering, Najafabad Branch, Islamic Azad University, Najafabad, Iran

Zhang et al. [14] explored the effects of Ag and Sc on the mechanical and microstructural properties of aluminum-copper alloys, specifically their influence on grain size. Their findings indicated that increasing the Sc content enhanced the UTS, elongation, and yield strength of the Al-Cu alloy.

Despite these advancements, gaps remain in understanding how varying temperature, strain rate, and copper content affect the mechanical properties of Al-Cu alloys, particularly in simulations that replicate real-world conditions under different loading scenarios. Theoretical and computational methods, such as molecular dynamics (MD), have proven highly effective in simulating material behaviors such as corrosion [15], reinforcement modulus [16], thermal conductivity [17], vibrational behavior [18], and mechanical properties [19, 20]. However, the application of MD simulations to Al-Cu alloys, especially considering the combined effects of temperature, strain rate, and copper content, remains underexplored.

Tiwary et al. [21] investigated the impact of layer thickness on the mechanical characteristics of the Al-Cu structure. They conducted this simulation using the Embedded Atom Method (EAM) interatomic potential. To achieve this, they utilized the NPT ensemble at 300 K, stabilized the system over 10,000-time steps, and extracted the stresses induced by tension. Ultimately, their study demonstrated the effect of layer thickness and structural influence on the stress-strain diagram.

Yanilkin et al. [22] examined the plastic behavior mechanisms of alloys under high-velocity loading at strain rates greater than  $10^5 \text{ s}^{-1}$ . They analyzed the alloy under these conditions using a multiscale approach, incorporating molecular dynamics (MD) simulations alongside a continuum mechanics model describing dislocation dynamics and elastic-plastic deformation. Dislocation velocities were calculated as functions of shear strength using molecular dynamics data across a wide temperature range up to the melting point. Stress-strain and shear strength diagrams were extracted from this simulation.

Meng et al. [23] conducted MD simulations of an Al-Cu alloy using a simulation box measuring  $162 \times 162 \times 405 \text{ \AA}^3$ , containing 640,000 atoms. The simulations incorporated periodic boundary conditions in the XY plane and employed an EAM potential to model atomic interactions among Cu-Cu, Al-Al, and Al-Cu atoms. However, there is still a need for comprehensive MD simulations that account for varying copper content, temperature, and strain rate, while also exploring their combined effects on the mechanical properties, such as UTS and elastic modulus, which are critical for the development of high-performance Al-Cu alloys.

In this study, the mechanical behavior of Al-Cu, one of the most significant alloys, was investigated. The Al-Cu alloy was simulated using molecular dynamics, and various properties were analyzed using this method [24, 25].

This study aims to fill these gaps by investigating the mechanical behavior of Al-Cu alloys using molecular dynamics simulations. Specifically, it examines how varying the volume percentage of copper, temperature, and strain rate influence the alloy's mechanical properties. The research also focuses on understanding the effects of temperature variations on misalignments, as well as the interaction between strain rate and copper content in shaping the alloy's ultimate strength and elastic modulus. Through this, the study seeks to provide insights that can guide the design of Al-Cu alloys with improved mechanical properties for various applications.

## Simulation method

The MD simulation is a computational method used to investigate the macroscopic characteristics of a system by analyzing its microscopic properties. Researchers define conditions that allow atoms within the system to interact over a specified period, enabling such studies. In molecular dynamics simulations, the motion of atoms is governed by Newton's equations of motion, which are expressed as follows:

$$F_i = m_i a_i = -\nabla_i U = -\frac{dU}{dr_i} \quad (1)$$

This computational approach allows molecules and atoms to interact within a defined timeframe, enabling the examination of complex systems with numerous components. To analyze the behavior of an aluminum-copper alloy under uniaxial tension, molecular dynamics simulation was performed using the LAMMPS software package.

The simulation incorporated periodic boundary conditions to mimic an infinitely repeating system. Interactions between copper and aluminum atoms were modeled using the EAM potential [26]. The EAM potential is a multi-body potential function used to represent interactions between particles. It accounts for all interatomic forces and the embedding energy of atoms, as described by the following function:

$$U_i = \sum_{i=1}^{N-1} \sum_{j=i+1}^N \phi(r_{ij}) + \sum_{i=1}^N F(\rho_i) \quad (2)$$

$$\rho_i = \sum_{i=1}^N \psi(r_{ij}) \quad (3)$$

$i$  and  $j$  represent interacting atoms among  $N$  total atoms, while  $r_{ij}$  denotes the distance between them. Moreover,  $\phi(r_{ij})$  and  $F(\rho_i)$  represent the interatomic energy and potential embedding function, respectively, both of which depend on the total electron density examined for the  $i$ -particle.

The dimensions of the simulation box for the Al-Cu alloy were set at  $512,000 \text{ \AA}^3$ . The NPT ensemble (where  $N$ ,  $P$ , and  $T$  represent the number of atoms, pressure, and temperature, respectively) was employed to ensure system equilibrium (Fig. 1). By carefully adjusting the parameters and using a 1-femtosecond time step, equilibrium was achieved within a relaxation period.

The mechanical properties, including the UTS and elastic modulus, were investigated under different conditions: temperatures of 300, 350, 400, 450, 500, and 600 K; strain rates of 0.001, 0.003, 0.005, 0.007, and  $0.01 \text{ ps}^{-1}$ ; ambient pressure of 100 kPa; and varying copper content percentages of 1%, 2%, 6%, 8%, 10%, 15%, and 20%.

The EAM potential parameters, including the equations governing interatomic interactions, were selected based on material-specific data from Ref. [26]. The system size was set at  $512,000 \text{ \AA}^3$ , with approximately 1.5 million atoms in total. The equilibration procedure consisted of two steps: first, the system was relaxed at constant temperature (300 K) and pressure (100 kPa) for 100,000 time steps, followed by adjusting the strain rate for mechanical testing. During equilibration, the temperature and pressure were maintained within 1% of the target values using the Nosé-Hoover thermostat and barostat. A time step of 1 femto-second was employed to ensure numerical stability and accurate results.

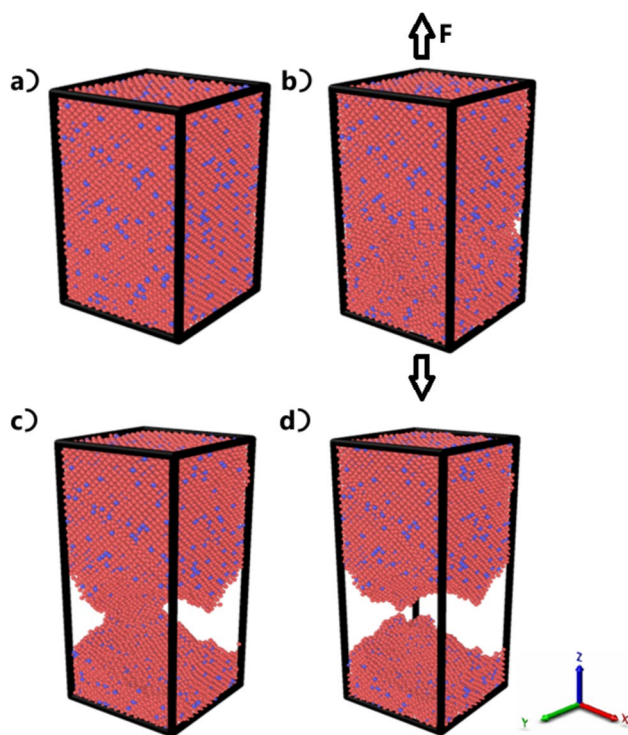


**Fig. 1** Initial loading stages leading to the failure of the Al-Cu alloy

## Results and discussion

### Temperature change effects

First, the effects of different temperatures (300 K, 350 K, 400 K, 450 K, 500 K, and 600 K) on the UTS and elastic modulus of an aluminum-copper alloy with 10% copper content (Al-Cu 10%) were investigated at a strain rate of  $0.001 \text{ ps}^{-1}$ . Figure 2 illustrates the stress–strain relationship at various temperatures for the 10% Cu alloy. The values of the elastic modulus and UTS of Al-Cu are presented in Table 1.

As shown in Table 1, the elastic modulus of the Al-Cu alloy decreased by 18.9% (from 60.098 to 48.743 GPa) as the temperature increased from 300 to 600 K. Additionally, the UTS declined by 31% (from 6.659 to 4.598 GPa) over the same temperature range. These results indicate that temperature has a significant impact on the mechanical properties of the Al-Cu alloy.

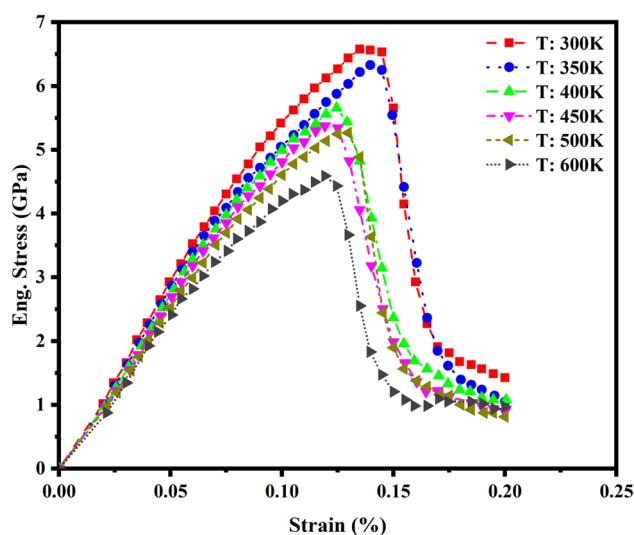


**Fig. 2** Stress–strain curve of Al-Cu (10%) alloy at various temperatures

**Table 1** Elastic modulus and the UTS of Al-Cu alloy at different temperatures

Temperature (K)	Elastic modulus (GPa)	Ultimate tensile strength (GPa)
300	60.098	6.659
350	59.09	6.323
400	56.323	5.646
450	54.627	5.384
500	51.683	5.286
600	48.743	4.598

In the MD simulations, the effects of temperature on the elastic modulus of nanocrystalline aluminum were investigated [27]. According to the findings, at a strain rate of  $0.001 \text{ ps}^{-1}$  and with simulation box dimensions of  $20 \times 10 \times 10 \text{ \AA}^3$ ,  $40 \times 20 \times 20 \text{ \AA}^3$ , and  $50 \times 25 \times 25 \text{ \AA}^3$ , the elastic modulus decreased by 12.049%, 12.027%, and 12.086%, respectively, as the temperature increased from 10 to 600 K. These results align with our findings.

### Strain rate effects

Strain rate is a critical parameter that significantly affects the mechanical characteristics of various materials. To calculate the strain rate, we first determine the strain:

$$\epsilon(t) = \frac{L(t) - L_0}{L_0} \quad (4)$$

where  $L(t)$  is the length at any time  $t$  and  $L_0$  is the original length. The strain rate is then calculated as follows:

$$\dot{\epsilon}(t) = \frac{d\epsilon}{dt} = \frac{d}{dt} \left( \frac{L(t) - L_0}{L_0} \right) = \frac{1}{L_0} \frac{dL(t)}{dt} = \frac{v(t)}{L_0} \quad (5)$$

where  $v(t)$  is the velocity at any given moment. In this part of the simulation, the effects of strain rate on the elastic modulus and the UTS of the Al-Cu (10%) alloy at 300 K were investigated. Various strain rates (i.e., 0.001, 0.003, 0.005, 0.007, and  $0.01 \text{ ps}^{-1}$ ) were examined for this purpose. Figure 3 illustrates the stress–strain curve of the Al-Cu (10%) alloy at different strain rates. Additionally, Table 2 presents the values of the elastic modulus and UTS for the Al-Cu (10%) alloy.

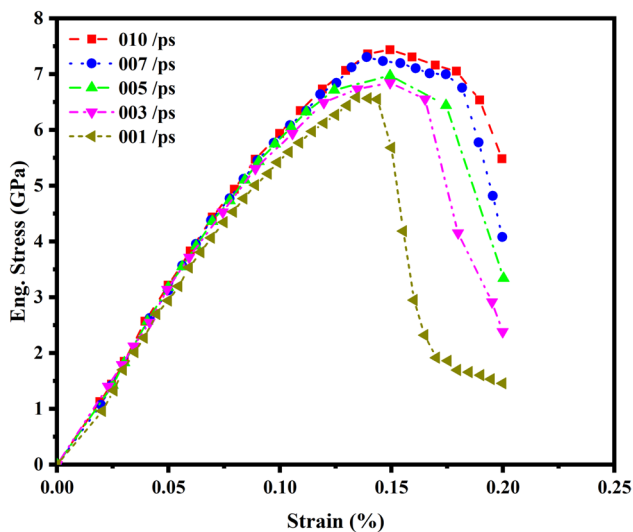


Fig. 3 Stress–strain vs. strain rates

**Table 2** Elastic and the UTS of Al-Cu alloy at various strain rates

Strain rate (1/ps)	Elastic modulus (GPa)	Ultimate tensile strength (GPa)
0.001	60.098	6.569
0.003	61.57	6.732
0.005	62.961	6.962
0.007	63.188	7.294
0.010	65.112	7.354

As shown in Table 2, as the strain rate increases from  $0.001 \text{ ps}^{-1}$  to  $0.01 \text{ ps}^{-1}$ , there is an observed increase of 8.343% in the elastic modulus and 11.95% in the UTS. Yu et al. [28] investigated the mechanical characteristics of the Al-Cu-Li alloy across different strain rates, demonstrating a relationship between higher strain rates and increased tensile strength. This conclusion is consistent with the findings of the present study.

### Effect of different percentages of copper

At this stage, the effects of varying copper percentages in the aluminum-copper alloy at 300 K and a strain rate of  $0.001 \text{ ps}^{-1}$  on the UTS and elastic modulus are investigated. Copper percentages of 1%, 2%, 6%, 8%, 10%, 15%, and 20% were used in this section. Figure 4 depicts the stress–strain curves of the Al-Cu alloy with different copper compositions. Table 3 presents data on the elastic modulus and UTS of the Al-Cu alloy at various copper percentages.

According to Table 3, the elastic modulus and UTS of the aluminum-copper alloy increase by 281% and 359%,

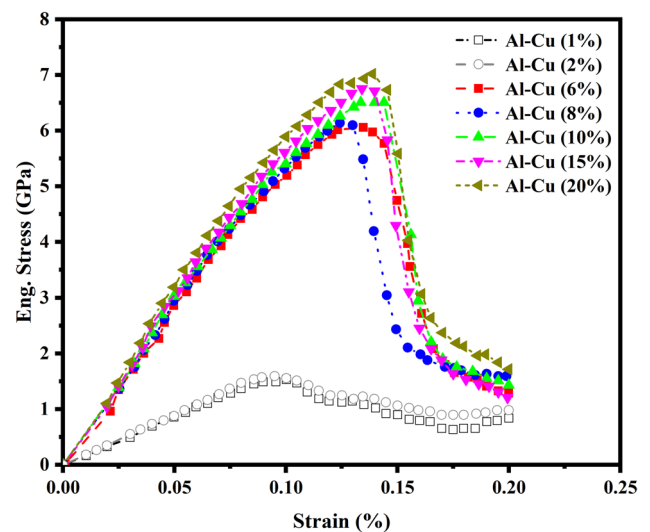


Fig. 4 Stress–strain curve of Al-Cu alloy with disparate percentages of copper

**Table 3** Properties of Al-Cu alloy with a variety of percentages of copper [29]

Cu content (%)	Elastic modulus (GPa)	Ultimate tensile Strength (GPa)
1%	17.101	1.538
2%	17.504	1.598
6%	57.98	6.093
8%	58.73	6.168
10%	60.098	6.569
15%	61.983	6.789
20%	65.207	7.059

respectively, when the copper percentage is increased from 1 to 20%. A significant 281% increase in the UTS of the Al-Cu alloy was observed when the copper percentage increased from 2 to 6%.

Xiao et al. [30] investigated the effect of various copper contents on the tensile strength of the Al-Cu-Mg-Ag alloy. The results indicated that increasing the copper percentage from 4 to 8% in the Al-Cu-Mg-Ag alloy significantly enhanced the tensile strength at 300 K and room temperature. Additionally, examining the influence of copper content on the UTS of the Al-Cu-Si-Mg alloy revealed that an increase in Cu content from 1 to 6% raised the tensile strength from 152 to 402 MPa, which is consistent with the results of this simulation [31].

### Statistical modelling and optimization

In the Design of Experiments (DOE), certain input factors, known as independent variables, are selected. Subsequently, simulations or empirical studies are conducted to derive outcomes, which serve as output factors, referred to as dependent variables in DOE, for optimization [32–34]. The Box-Behnken design (BBD) is employed as the experimental strategy. Strain rate and temperature are considered at three levels each, while copper content is varied across four levels, as shown in Table 4.

Table 5 shows the values of the output variables for 15 simulations under various conditions. In Table 5, T, S, C, and E represent ambient temperature, strain rate, copper content in the aluminum matrix, and elastic modulus, respectively.

### The mathematical modelling for elastic modulus

The mathematical model for the elastic modulus is proposed through analysis of variance (ANOVA). The results of the ANOVA for the elastic modulus are presented in Table 6. Furthermore, the mathematical model for the elastic modulus is shown as follows:

**Table 4** Modulus and the UTS of Al-Cu alloy with a variety of percentages of copper

Input parameters	Levels
Temperature, K	300
Strain rate, 1/ps	0.001
Content, %	2
	6
	10
	20
	600
	0.01



**Table 5** The output variables

Run	T (K)	S (1/ps)	C (%)	E (GPa)	UTS (GPa)
1	300	0.001	2	17.504	1.598
2	450	0.001	10	54.627	5.384
3	300	0.01	10	65.112	7.354
4	300	0.005	10	62.961	6.962
5	300	0.001	6	57.98	6.093
6	300	0.001	10	60.098	6.569
7	600	0.001	10	48.743	4.598
8	450	0.001	10	54.627	5.384
9	600	0.001	10	48.743	4.598
10	300	0.005	10	62.961	6.962
11	300	0.01	10	65.112	7.354
12	300	0.001	20	65.207	7.059
13	450	0.001	10	54.027	5.384
14	300	0.001	20	65.207	7.059
15	300	0.01	10	63.112	7.354

**Table 6** Analysis of variance for elastic modulus

Source	DF	Adj SS	Adj MS	F-Value	P-Value
Model	7	1958.78	279.826	14.24	0.001
Linear	3	1271.00	423.666	21.56	0.001
T	1	259.85	259.855	13.23	0.008
S	1	3.33	3.334	0.17	0.693
C	1	734.41	734.407	37.38	0.000
Square	3	590.23	196.745	10.01	0.000
T*T	1	15.71	15.708	0.80	0.006
S*S	1	8.52	8.523	0.43	0.401
C*C	1	509.23	509.225	25.92	0.001
2-Way Interaction	1	2.62	2.616	0.13	0.726
S*C	1	2.62	2.616	0.13	0.726
Error	7	137.54	19.648		
Lack-of-Fit	1	134.63	134.630	277.91	0.000
Pure Error	6	2.91	0.484		
Total	14	2096.32			

**R-sq** = 93.44%, **R-sq(adj)** = 86.88%

$$E = 47.9 - 0.185 T - 1949 S + 9.56 C + 0.000140 T * T + 129,144 S * S - 0.3265 C * C + 30.9 S * C \quad (6)$$

where  $T$  is the temperature in Kelvin,  $C$  is the copper content in percent, and  $S$  is the strain rate in picoseconds. As observed, the value of  $E$  can be calculated as a function of temperature, copper content, and strain rate.

According to the analysis of variance for the elastic modulus, the confidence interval is 95% because the p-value in Table 6 is significantly less than 5%. Moreover, the correlation coefficients  $R^2$  and adjusted  $R^2$  are

93.44% and 86.88%, respectively, indicating a good fit for the mathematical model of the elastic modulus proposed by the ANOVA method.

### The mathematical modelling for ultimate strength

In this section, the mathematical model for the UTS is presented as follows:

$$UTS = 6.77 - 0.0294 T - 146 S + 1.111 C + 0.000023 T * T + 15,489 S * S - 0.03775 C * C - 0.75 S * C \quad (7)$$

where  $S$  is the strain rate in picoseconds,  $T$  is the ambient temperature in Kelvin,  $C$  is the copper content in percent, and UTS is in GPa. Table 7 shows the ANOVA results for the UTS.

From Table 7, it can be observed that the probability value for the UTS is significantly less than 5%, which is desirable. Additionally, the correlation coefficients  $R^2$  and adjusted  $R^2$  for this model are 96.03% and 92.05%, respectively, demonstrating the accuracy and adequacy of the model.

In this study, the optimization aims to maximize both the UTS and modulus of elasticity using the desirability approach pioneered by Derringer et al. [35]. The maximization of these mechanical properties is depicted in Fig. 5. Examination of the figure reveals that at a temperature of 300 K, a strain rate of 0.01, and a copper content of 14.5455%, the UTS and elastic modulus reach their peak values. According to the findings, the maximum predicted values for the UTS and elastic modulus are 8.1559 GPa and 72.8873 GPa, respectively. Subsequently, to validate

**Table 7** Analysis of variance for ultimate tensile strength

Source	DF	Adj SS	Adj MS	F-Value	P-Value
Model	7	33.0022	4.71460	24.17	0.000
Linear	3	21.4208	7.14028	36.60	0.000
T	1	5.6545	5.65452	28.98	0.001
S	1	0.0230	0.02305	0.12	0.741
C	1	8.6002	8.60022	44.08	0.000
Square	3	7.6526	2.55085	13.07	0.003
T*T	1	0.4232	0.42319	2.17	0.184
S*S	1	0.1226	0.12259	0.63	0.454
C*C	1	6.8072	6.80723	34.89	0.001
2-Way Interaction	1	0.0015	0.00152	0.01	0.932
S*C	1	0.0015	0.00152	0.01	0.932
Error	7	1.3657	0.19510		
Lack-of-Fit	1	1.3657	1.36567	*	*
Pure Error	6	0.0000	0.00000		
Total	14	34.3679			

**R-sq** = 96.03%, **R-sq(adj)** = 92.05%

**Fig. 5** The optimal modulus and the UTS proposed by Derringer method

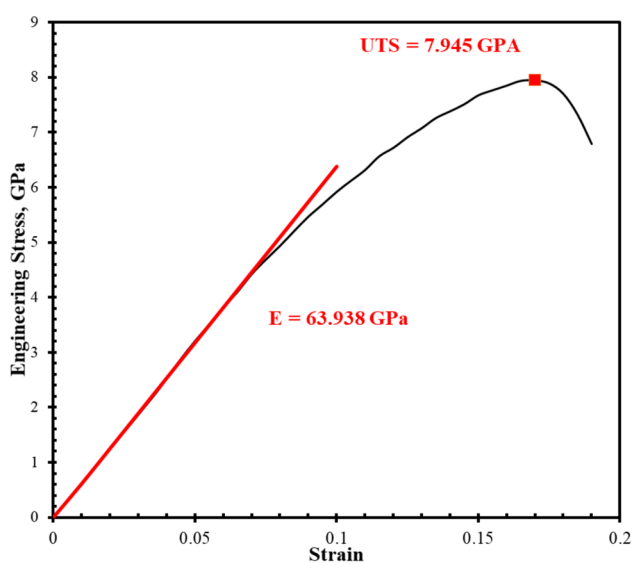
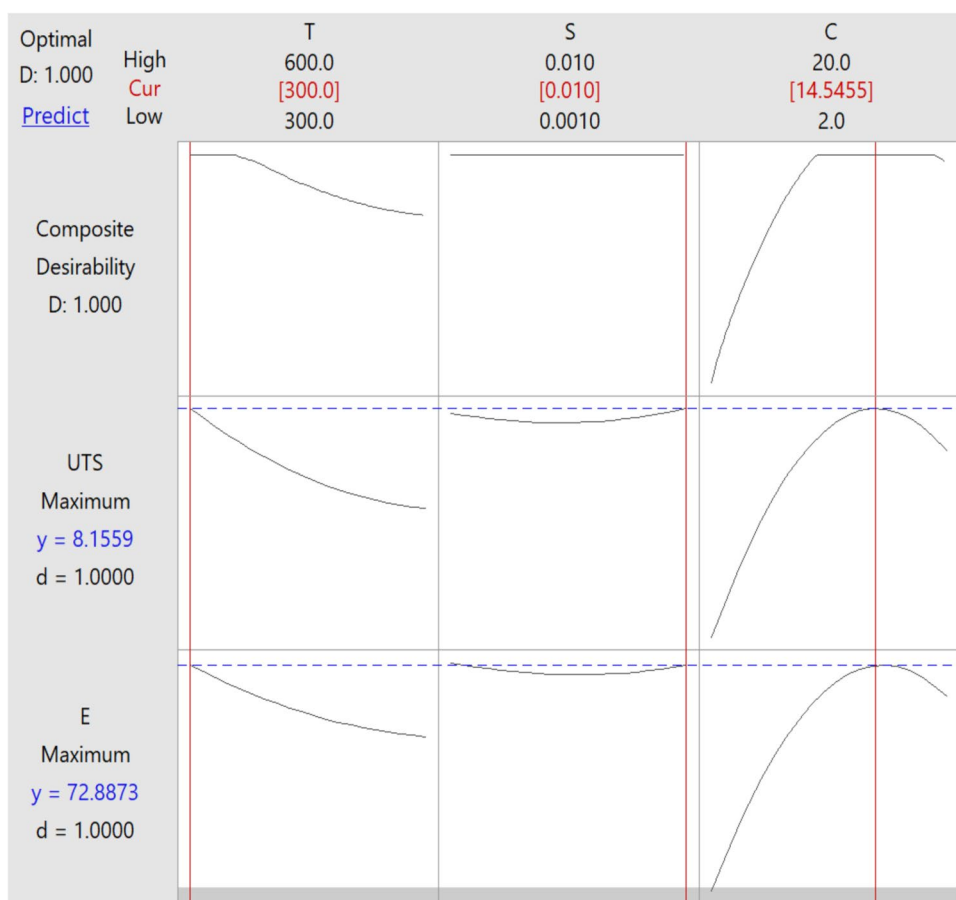


**Fig. 6** Stress–strain curve of Al-Cu alloy for proposed model

these predicted maxima, simulations were conducted under the specified conditions ( $T = 300$  K,  $S = 0.01$ , and  $C = 14.5455\%$ ), as illustrated in Fig. 6. Here, the computed values for Young's modulus and the UTS were 63.938 GPa

and 7.945 GPa. The accuracy of the predicted values was found to be 86.003% for the elastic modulus and 97.345% for the UTS, indicating the reliability and desirability of the proposed model.

As the temperature increases, the reduction in both the elastic modulus and ultimate tensile strength (UTS) can be attributed to the thermal activation of atomic vibrations, which cause a softening of the material. At higher temperatures, atomic mobility increases, leading to a decrease in the material's resistance to deformation, thereby lowering its mechanical strength. This trend is consistent with previous studies, such as those by Li et al. [27], which observed similar reductions in the elastic modulus of aluminum alloys at elevated temperatures.

The strain rate dependence is linked to the rate of dislocation movement and the material's ability to resist deformation. At higher strain rates, dislocations do not have enough time to overcome obstacles and are unable to move freely, resulting in an increase in the material's strength. This is reflected in the observed rise in both the elastic modulus and UTS with increased strain rates. The same behavior was observed by Yu et al. [28] in Al-Cu alloys, reinforcing the idea that higher strain rates lead to stronger material behavior due to the suppression of dislocation motion.

Regarding the copper content, the increase in copper percentage in the Al-Cu alloy leads to enhanced mechanical properties, which can be explained by the formation of solid solution strengthening. Copper atoms, being larger than aluminum atoms, create lattice distortions that impede the movement of dislocations, thus increasing both the elastic modulus and UTS. This effect becomes more pronounced at higher copper contents, as shown by the significant increases in mechanical properties when copper content rises from 1 to 20%, consistent with findings by Xiao et al. [30] and Zeren [31].

While the primary focus of this study was on solid solution hardening, which is the dominant mechanism influencing the mechanical properties of the Al-Cu alloy in this simulation, precipitation hardening could also contribute to the observed material strengthening, especially at higher copper concentrations. Precipitation hardening, which involves the formation of fine precipitates within the alloy matrix, can further enhance tensile strength and hardness by impeding dislocation movement. Although this mechanism was not explicitly incorporated into the present simulations, it is an important consideration, particularly in alloys with higher copper content.

## Conclusion

Alloys are materials produced to achieve enhanced mechanical properties. Finding the optimal combination of metals in alloys for superior mechanical performance has been the focus of extensive research. This study investigates the mechanical behavior of an aluminum-copper alloy. Molecular dynamics simulations were used to explore how varying the volume percentage of copper, temperature, and strain rate affect the alloy and its mechanical properties.

This simulation method is highly accurate and closely mimics experimental techniques. The use of theoretical and computational methods to explore the influence of various variables on alloy properties has been considered for several years. Lower costs, the ability to study multiple variables without restrictions on the number of tests, and the avoidance of advanced and expensive laboratory equipment have made computational methods highly attractive. Among these methods, molecular dynamics stands out as one of the best for simulating materials and investigating their mechanical properties.

The results show that increasing the volume percentage of copper from 1 to 20% significantly enhances both the UTS and elastic modulus. Additionally, increasing the temperature from 300 to 600 K decreases the elastic modulus by 19% and the UTS by approximately 31%. Regarding the strain rate, increasing it from 0.001 ps<sup>-1</sup> to 0.01 ps<sup>-1</sup> results in an 8.343% increase in the modulus of elasticity and an

11.95% increase in the UTS. These findings indicate that the best mechanical properties of the alloy are achieved by using a higher percentage of copper and reducing the operating temperature at an appropriate strain rate.

Using the RSM approach, maximum values of 8.1559 GPa and 72.8873 GPa were predicted for the UTS and elastic modulus, respectively. Verification of these maximum predicted values for the elastic modulus and UTS showed prediction accuracies of 86.003% and 97.345%, respectively.

Future work could aim to model and investigate the combined effects of solid solution and precipitation hardening in Al-Cu alloys to provide a more comprehensive understanding of their mechanical behavior across different copper contents and temperature conditions.

**Authors' contribution** Mostafa Yazdani, Aazam Ghassemi, Mohamad Shahgholi, Javad Jafari Fesharaki, Seyed Ali Galehdari wrote the main manuscript text and they all (Mostafa Yazdani, Aazam Ghassemi, Mohamad Shahgholi, Javad Jafari Fesharaki, Seyed Ali Galehdari) prepared the all figures. All authors (Mostafa Yazdani, Aazam Ghassemi, Mohamad Shahgholi, Javad Jafari Fesharaki, Seyed Ali Galehdari) reviewed the manuscript.

**Funding** There is no funding.

**Data availability** No datasets were generated or analysed during the current study.

## Declarations

**Conflict of interest** The authors declare no competing interests.

## References

1. Tang YT, Panwisawas C, Ghoussoub JN, Gong Y, Clark JW, Németh AA, Reed RC (2021) Alloys-by-design: Application to new superalloys for additive manufacturing. *Acta Mater* 202:417–436. <https://doi.org/10.1016/j.actamat.2020.09.023>
2. Qin Z, Wang Z, Wang Y, Zhang L, Li W, Liu J, Liu Y (2021) Phase prediction of Ni-base superalloys via high-throughput experiments and machine learning. *Materials Research Letters* 9(1):32–40. <https://doi.org/10.1080/21663831.2020.1815093>
3. Zhang Y, Xu X (2021) Lattice misfit predictions via the Gaussian process regression for Ni-based single crystal superalloys. *Met Mater Int* 27(2):235–253. <https://doi.org/10.1007/s12540-020-00883-7>
4. Strickland J, Nenchev B, Tassenberg K, Perry S, Sheppard G, Dong H, D'Souza N (2021) On the origin of mosaicity in directionally solidified Ni-base superalloys. *Acta Mater* 217:117180. <https://doi.org/10.1016/j.actamat.2021.117180>
5. Makineni SK, Singh MP, Chattopadhyay K (2021) Low-density, high-temperature Co base superalloys. *Annu Rev Mater Res* 51. <https://doi.org/10.1146/annurev-matsci-080619-014459>
6. Zhang J, Huang T, Cao K, Chen J, Zong H, Wang D, Liu L (2021) A correlative multidimensional study of  $\gamma'$  precipitates with Ta addition in Re-containing Ni-based single crystal superalloys. *J Mater Sci Technol* 75:68–77. <https://doi.org/10.1016/j.jmst.2020.10.025>



7. Katnagallu S, Vernier S, Charpagne MA, Gault B, Bozzolo N, Kontis P (2021) Nucleation mechanism of hetero-epitaxial recrystallization in wrought nickel-based superalloys. *Scripta Mater* 191:7–11. <https://doi.org/10.1016/j.scriptamat.2020.09.012>
8. Gupta S, Bronkhorst CA (2021) Crystal plasticity model for single crystal Ni-based superalloys: Capturing orientation and temperature dependence of flow stress. *Int J Plast* 137:102896. <https://doi.org/10.1016/j.ijplas.2020.102896>
9. Yu Q, Wang C, Zhao Z, Dong C, Zhang Y (2021) New Ni-based superalloys designed for laser additive manufacturing. *J Alloy Compd* 861:157979. <https://doi.org/10.1016/j.jallcom.2020.157979>
10. Liu G, Du D, Wang K, Pu Z, Chang B (2021) Epitaxial growth behavior and stray grains formation mechanism during laser surface re-melting of directionally solidified nickel-based superalloys. *J Alloy Compd* 853:157325. <https://doi.org/10.1016/j.jallcom.2020.157325>
11. Wang Z, Lin X, Wang L, Cao Y, Zhou Y, Huang W (2021) Microstructure evolution and mechanical properties of the wire+ arc additive manufacturing Al-Cu alloy. *Addit Manuf* 47:102298. <https://doi.org/10.1016/j.addma.2021.102298>
12. Mair P, Kaserer L, Braun J, Weinberger N, Letofsky-Papst I, Leichtfried G (2021) Microstructure and mechanical properties of a TiB<sub>2</sub>-modified Al-Cu alloy processed by laser powder-bed fusion. *Mater Sci Eng, A* 799:140209. <https://doi.org/10.1016/j.msea.2020.140209>
13. Milligan B, Ma D, Allard L, Clarke A, Shyam A (2021) Crystallographic orientation-dependent strain hardening in a precipitation-strengthened Al-Cu alloy. *Acta Mater* 205:116577. <https://doi.org/10.1016/j.actamat.2020.116577>
14. Zhang M, Wang J, Wang B, Xue C, Liu X (2022) Quantifying the effects of Sc and Ag on the microstructure and mechanical properties of Al-Cu alloys. *Mater Sci Eng, A* 831:142355. <https://doi.org/10.1016/j.msea.2021.142355>
15. Eskandari M, Yeganeh M, Motamedi M (2012) Investigation in the corrosion behaviour of bulk nanocrystalline 316L austenitic stainless steel in NaCl solution. *Micro & Nano Letters* 7(4):380–383. <https://doi.org/10.1049/mnl.2012.0162>
16. Motamedi M, Eskandari M, Yeganeh M (2012) Effect of straight and wavy carbon nanotube on the reinforcement modulus in non-linear elastic matrix nanocomposites. *Mater Des* 34:603–608. <https://doi.org/10.1016/j.matdes.2011.05.013>
17. Motamedi M, Safdari E, Nikzad M (2021) Effect of different parameters on the heat transfer coefficient of silicon and carbon nanotubes. *Int Commun Heat Mass Transfer* 129:105692. <https://doi.org/10.1016/j.icheatmasstransfer.2021.105692>
18. Motamedi M, Mashhadi MM, Rastgoo A (2013) Vibration behavior and mechanical properties of carbon nanotube junction. *J Comput Theor Nanosci* 10(4):1033–1037. <https://doi.org/10.1166/jctn.2013.2803>
19. Motamedi M, Mehrvar A, Nikzad M (2023) Statistical modelling and optimization of AL/CNT composite using response surface-desirability approach. *Comput Part Mech* :143–153. <https://doi.org/10.1007/s40571-022-00484-8>
20. Motamedi M, Mehrvar A, Nikzad M (2022) Mechanical properties of aluminum/SiNT nanocomposite. *Proc Inst Mech Eng C: J Mech Eng Sci* :09544062221112798. <https://doi.org/10.1177/09544062221112798>
21. Tiwary CS, Chakraborty S, Mahapatra DR, Chattopadhyay K (2014) Length-scale dependent mechanical properties of Al-Cu eutectic alloy: molecular dynamics based model and its experimental verification. *J Appl Phys* 115(20):203502. <https://doi.org/10.1063/1.4879249>
22. Yanilkin AV, Krasnikov VS, Kuksin AY, Mayer AE (2014) Dynamics and kinetics of dislocations in Al and Al-Cu alloy under dynamic loading. *Int J Plast* 55:94–107. <https://doi.org/10.1016/j.ijplas.2013.09.008>
23. Meng X, Zhou J, Huang S, Su C, Sheng J (2017) Properties of a laser shock wave in Al-Cu alloy under elevated temperatures: A molecular dynamics simulation study. *Materials* 10(1):73. <https://doi.org/10.3390/ma10010073>
24. Trybula ME, Szafranski PW, Korzhavyy PA (2018) Structure and chemistry of liquid Al-Cu alloys: molecular dynamics study versus thermodynamics-based modelling. *J Mater Sci* 53(11):8285–8301. <https://doi.org/10.1007/s10853-018-2116-8>
25. Li C, Li D, Tao X, Chen H, Ouyang Y (2014) Molecular dynamics simulation of diffusion bonding of Al-Cu interface. *Modell Simul Mater Sci Eng* 22(6):065013. <https://doi.org/10.1088/0965-0393/22/6/065013>
26. Mojumder S (2018) Molecular dynamics study of plasticity in Al-Cu alloy nanopillar due to compressive loading. *Physica B* 530:86–89. <https://doi.org/10.1016/j.physb.2017.10.119>
27. Li Z, Gao Y, Zhan S, Fang H, Zhang Z (2020) Molecular dynamics study on temperature and strain rate dependences of mechanical properties of single crystal Al under uniaxial loading. *AIP Adv* 10(7):075321. <https://doi.org/10.1063/1.5086903>
28. Yu H, Jin Y, Hu L, Wang Y (2020) Mechanical properties of the solution treated and quenched Al-Cu-Li alloy (AA2195) sheet during high strain rate deformation at room temperature. *Mater Sci Eng, A* 793:139880. <https://doi.org/10.1016/j.msea.2020.139880>
29. Yazdani M, Ghassemi A, Shahgholi M, Fesharaki JJ, Galehdari SA (2025) Comparing mechanical properties of AL/Cu composite obtained by Mori-Tanaka and dynamic molecular methods. *J Adv Mater Proc*. Paper ID 202411061189702. Article in Press
30. Xiao DH, Wang JN, Ding DY, Chen SP (2002) Effect of Cu content on the mechanical properties of an Al-Cu-Mg-Ag alloy. *J Alloy Compd* 343(1–2):77–81. [https://doi.org/10.1016/S0925-8388\(02\)00076-2](https://doi.org/10.1016/S0925-8388(02)00076-2)
31. Zeren M (2005) Effect of copper and silicon content on mechanical properties in Al-Cu-Si-Mg alloys. *J Mater Process Technol* 169(2):292–298. <https://doi.org/10.1016/j.jmatprotec.2005.03.009>
32. Gunst RF (1996). Response surface methodology: process and product optimization using designed experiments. <https://doi.org/10.1080/00401706.1996.10484509>
33. Nemeth MA (2003) Response surface methodology: Process and product optimization using designed experiments. *J Qual Technol* 35(4):428. <https://doi.org/10.1080/00224065.2003.11980243>
34. Jensen WA (2017) Response surface methodology: process and product optimization using designed experiments. *J Qual Technol* 49(2):186. <https://doi.org/10.1080/00224065.2017.11917988>
35. Derringer G, Suich R (1980) Simultaneous optimization of several response variables. *J Qual Technol* 12(4):214–219. <https://doi.org/10.1080/00224065.1980.11980968>

**Publisher's Note** Springer Nature remains neutral with regard to jurisdictional claims in published maps and institutional affiliations.

Springer Nature or its licensor (e.g. a society or other partner) holds exclusive rights to this article under a publishing agreement with the author(s) or other rightsholder(s); author self-archiving of the accepted manuscript version of this article is solely governed by the terms of such publishing agreement and applicable law.